Carbon-Assisted Growth of SiO_x Nanowires

S.-H. Li, X.-F. Zhu, and Y.-P. Zhao*

Department of Physics and Astronomy, Nanoscale Science and Engineering Center, The University of Georgia, Athens, Georgia 30602

Received: April 9, 2004; In Final Form: July 1, 2004

During attempts to fabricate ZnO nanowires, we accidentally observed the growth of SiO_x nanowires on Au-coated Si substrate. Detailed characterizations on the resulting nanowires were carried out by field-emission scanning electron microscopy, electron microprobe analysis, transmission electron microscopy, selective area electron diffraction, energy-dispersed X-ray spectroscopy, X-ray diffraction, and X-ray photoelectron spectroscopy. The resulting nanowires have a Si-to-O ratio of 1:1.63 and a diameter of 50−300 nm. It was found that the presence of graphite powder in the growth furnace was critical. A systematic investigation of how the growth conditions, such as the growth temperature, the oxygen-to-Ar carrier gas ratio, and growth time, affect the formation of SiO_x nanowires was performed. Higher growth temperature and appropriate low oxygen gas flow helped to promote long nanowire growth. The diameters of the nanowires increased with growth time. It was demonstrated that the formation of the SiO_x nanowires was due to a solid−liquid−solid mechanism, and the locally catalytic oxidation of CO by Au nanoclusters may play a role in accelerating nanowire formation.

I. Introduction

One-dimensional SiO_x nanowires have recently attracted considerable research attention due to their unique optical properties and promising applications.[1−19] The stable and bright blue emission of SiO_x nanowires makes them potential sources of high-intensity light, near-field optical microscope probes, waveguides, etc. So far, many different methods have been employed to fabricate these nanowires, and different growth mechanisms have been proposed. In general, there are two different fabrication approaches: non-catalyst-based and catalyst-based methods. Only a few papers have been devoted to the non-catalyst-based method.[1−6] In this case, usually Si wafers,[1−4] SiO_2 nanoparticles,[5] and a mixture of Si and SiO_2 powder[6] were used as the source materials, and the oxygen came from either the O_2 gas flow[1−3] or the source materials (e.g., SiO_2)[5,6] or was attributed to the residue O_2 gas in the chamber or carrier gas.[4] The nanowire formation temperatures were usually over 1000 °C, and the growth time was very long (≥1 h). The growth mechanisms for the noncatalyst method are not yet well understood. The majority of SiO_x nanowire fabrication methods are catalyst-based methods. Different kinds of catalysts have been used, such as Au,[7−9] Fe,[10−14] Co,[15,16] Ni,[17] Ge,[18−20] and other metal alloys.[21] In most cases, the formation of SiO_x nanowires has been attributed to a vapor−liquid−solid mechanism:[22] a nanocluster serves as the critical point for nucleation, and the addition of reactants from the vapor phase allows the formation of a nanowire underneath the catalyst cluster. So far, there are three papers that have reported carbon-assisted SiO_x nanowire growth.[16,23,24] But the opinions on the nanowire formation mechanism are controversial. Zu et al. have reported the formation of SiO_2 nanoflowers by mixing SiC and cobalt powders when heated to 1500 °C. They used a graphite heater, and concluded that the CO liberated from the graphite heater played an important role. They demonstrated that SiO_2 nanowires can be grown successfully by the direct flow of CO gas (mixed with Ar) into the chamber.[23] Carter et al. also showed crystalline SiO_2 nanofibers grown from the Ni−Si and Co−Si alloy surface by exposing the alloys to Ar/CO_2 and $Ar/CO/CO_2$ gases at 1130 °C. They proposed that CO_2, not O_2, nor CO, was the decisive factor for the growth through the following reaction:[16]

$$CO_2(g) + Si(s) \rightarrow CO + SiO(g) \quad (1)$$

Saulig-Wenger et al. have reported the synthesis of amorphous silicon dioxide nanowires with the presence of graphite in the furnace.[24] The source materials were Si powder (no Au), the $Ar:O_2$ carrier gas ratio was 99.2 mol %:0.8 mol %, and the growth temperature was 1200 °C. They found the relative O_2 flow rate played a very important role in the formation of the nanowires: having either no O_2 or a large amount of O_2 did actually hinder the nanowire growth. They postulated a nanowire growth mechanism similar to that of Carter et al.[24,16]

Here we describe the carbon-assisted method to synthesize SiO_x nanowires with a short growth time (∼30 min) on Au-coated Si substrates. The method was found accidentally during our attempts to fabricate ZnO nanowires, and was similar to methods reported recently.[16,23,24] We will present a detailed study on how different growth conditions affect the SiO_x nanowire growth. The results show that the possible growth mechanism for nanowire formation is the solid−liquid−solid (SLS) process.

II. Experiments

The attempted ZnO nanowire fabrication follows the thermal-carbon reduction method reported in the literature.[25−27] The growth equipment consisted of a 2 in. diameter quartz tube, a three-zone hinged furnace (Lindeberg Blue M), two flow controllers (MKS 1179A) with a power supply (MKS 247D), and a mechanical pumping system. As reported in the literatures, the source was a mixture of 2.5 g of ZnO powder (99.99%, −325 mesh, Alfa Aesar) and 2.5 g of graphite powder (99.6%, −325 mesh, Alfa Aesar). The powders were mixed by mechan-

10.1021/jp048418x CCC: $27.50
Published on Web 10/08/2004

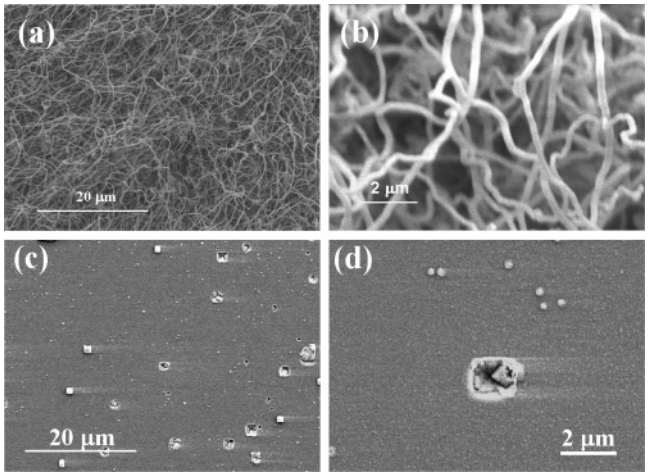

Figure 1. Representative SEM images of the nanowires on Au−Si substrate (a, b) and pits/hillocks on Cu−Si substrate (c, d) with a mixture of ZnO and graphite powders as the source. Image b is the zoom-in of image a, and image d is the zoom-in of image c.

ical milling for 15 min, and then placed in a quartz boat. Throughout all the experiments, three different kinds of substrates were placed side-by-side in the furnace: a 6.4 nm thick gold film on Si(100) substrate (AUS), a 10 nm thick Cu film on Si(100) substrate (CUS), and a bare Si(100) substrate (BS). No further annealing to the substrates was performed before they were put into the furnace. The source was placed in the center of the tube furnace, while the substrates were placed in another quartz boat, 2 in. downstream. The quartz tube was first evacuated to a background pressure of 10 mTorr at room temperature, and then backfilled with Ar (99.998%) gas to achieve a pressure of 14 Torr. With a constant 300 sccm of Ar flow, the quartz-tube chamber was rapidly heated (with a rate of 80 °C/min) to predetermined temperatures set by the furnace controller, 900, 950, 1000, and 1100 °C, respectively. The pressure during growth was kept from 60 to 800 Torr. The synthesis duration usually was 30 min. After deposition, the furnace was turned off and the chamber was cooled naturally to room temperature with Ar protection. When opening the chamber, we observed that there was a layer of gray film (Zn) covering the inside of the cold section of the quartz tube at all four different temperatures. A layer of thin white (sometimes light gray) products was found covering the AUS substrates, while there were no white powders on both CUS and BS. When examined with a Mituyoko optical microscope (1000×, dark-field), we observed fine hairlike wires on the AUS surfaces and no hairlike wires on both CUS and BS substrates. Detailed characterizations on the resulting wires on AUS were carried out by field-emission scanning electron microscopy (SEM; LEO 982, FEG), transmission electron microscopy (TEM; Tecnai 20), electron microprobe analysis (JEOL JXA 8600), energy-dispersed X-ray spectroscopy (EDS), X-ray diffraction (XRD), and X-ray photoelectron spectroscopy (XPS).

III. Experimental Results

1. SiO_x Nanowire Formed by a ZnO and Graphite Powder Mixture. Figure 1 shows the SEM top views of the morphology on AUS and CUS substrates after the deposition. There are randomly tangled nanowires presented on the AUS substrate, while on CUS there are randomly distributed square-shaped pits or hillocks, and no nanowires are observed. Unlike the straight crystalline ZnO nanowires produced in the literature,[25] these long nanowires on AUS substrate are entangled together and

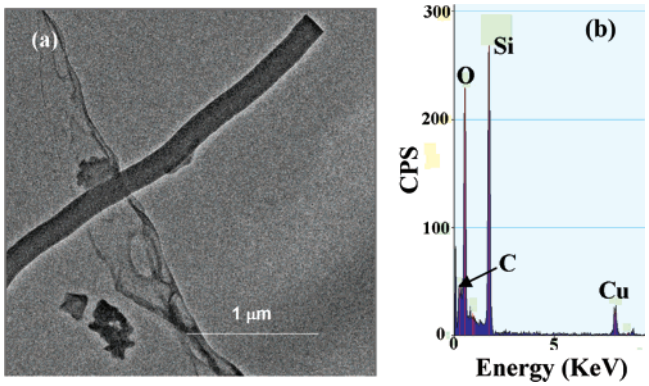

Figure 2. (a) TEM image and (b) EDS spectrum of the representative nanowire fabricated using a mixture of ZnO and graphite powders. There are two very strong peaks of Si and O in the EDS spectrum. The background in the TEM image is the carbon film on the grid.

form a nanowire network. Depending on the growth conditions, the diameters of the nanowires vary from 50 to 300 nm. The distinct morphological difference between the nanowires we obtained and the ZnO nanowires reported in the literature raised our suspicions on the chemical constitution of those nanowires. To obtain the compositions of the nanowires, we performed TEM, EDS, XPS, and microprobe experiments. Figure 2 shows the TEM and EDS results. For the TEM observation presented in Figure 2a, the nanowires were scraped off from the Si substrate by a razor blade, ultrasonically detangled in acetone, and dispersed onto the lacy carbon film on the Cu grid (from Ernest F. Fullam, Co.). The EDS spectrum (Figure 2b) shows two very distinct peaks of Si and O. The Cu peaks come from the TEM Cu grid, and the C peak partially comes from the carbon film on the TEM grid, and partially could come from the graphite powder in the source. Neither Au nor Zn was found in the nanowires within the detection limits. The nanowires contained a large amount of Si and O. Selective area diffraction on a single nanowire and X-ray diffraction on a layer of nanowires on a Si wafer did not reveal any characterization crystalline peaks, which demonstrated the wires were amorphous structures. We further confirmed the EDS results by XPS. Figure 3 shows the XPS results obtained from the same sample. There are almost no C peaks present in the spectrum (no C 1s peak at 284.3 eV as shown in Figure 3a). The finer resolution XPS spectra showed that the Si 2p peak is located at 104.4 eV, while the O 1s peak is located at 533.8 eV. These two peaks are the characteristic peaks for SiO_2 (due to the surface charging effect, all the XPS peaks have a +1 eV shift with respect to those of the standard XPS SiO_2 spectra). Nevertheless, there is no Si peak at 99.2 eV (bulk Si XPS peak), which means the resulting XPS spectra are from the top layer of the film. Quantitative analysis of the Si 2p and O 1s peaks gives the Si-to-O ratio to be 1:1.63. XPS spectra also reveal that there are no Au and Zn present at the nanowire layer within the detection limits. In fact, occasionally we could find ZnO tetrapod structures on the surface. Figure 4 shows the electron microprobe mapping of one portion of the sample. Figure 4a is the morphology of the surface we scanned, while Figure 4b is the map of the Zn element of the same surface. We can clearly see the tetrapod structures associated with high Zn concentration.

The above observations and experimental results show that, after thermal-carbon reduction of ZnO, most of the Zn did not react with Au or Au−Si alloy on the substrate to form ZnO nanowires, as expected from the literature.[25−27] Instead, the reaction promoted the formation of SiO_x nanowires within a short reaction time (30 min). Under our experimental setup, the

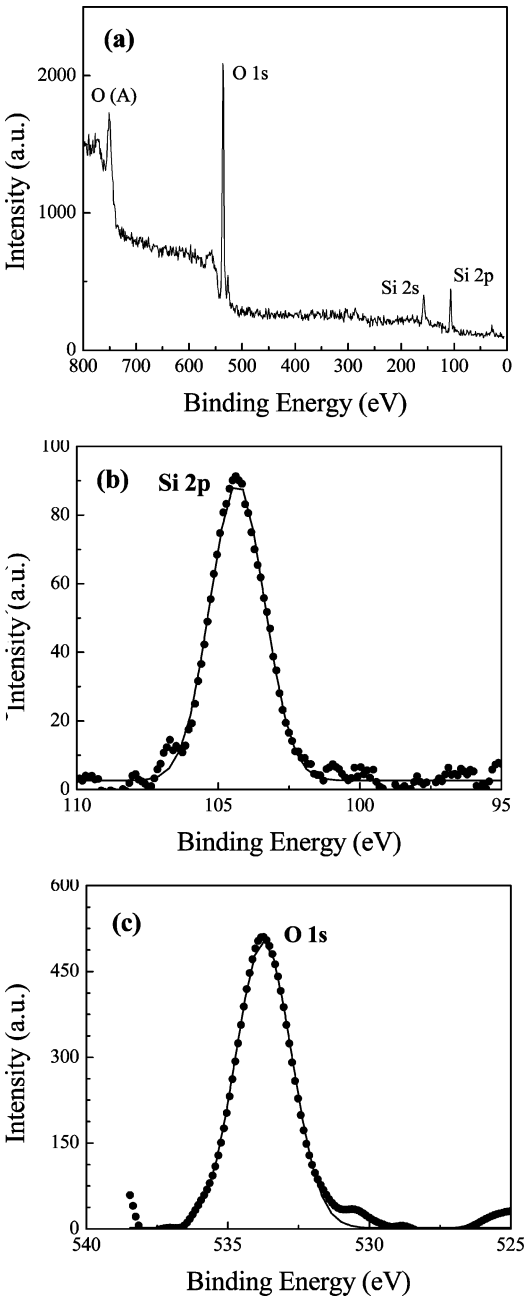

Figure 3. XPS spectra of the nanowire film fabricated using a mixture of ZnO and graphite powders: (a) survey spectrum; (b) Si 2p spectrum; (c) O 1s spectrum. The solid curves in b and c are the best Gaussian fittings for the two peaks.

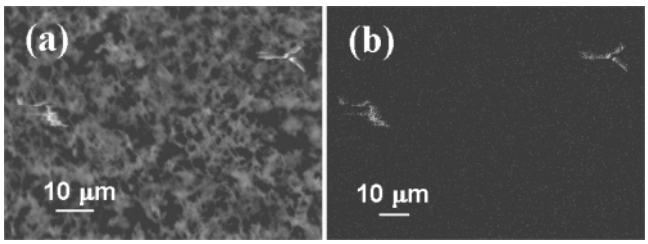

Figure 4. Electron microprobe analysis of the nanowire film fabricated using a mixture of ZnO and graphite powders: (a) electron microprobe morphological image; (b) Zn element mapping of (a).

vapor pressure of Zn was not high enough to induce ZnO nanowire formation through the VLS mechanism.

The most unexpected result from the above experiments was the formation of the amorphous SiO_x nanowires on Au-coated substrates. These results were quite different from those reported in the literature, where the SiO_x nanowires were formed at higher temperature and for longer reaction time.[1−22] To understand the growth mechanism of SiO_x nanowires, we have performed a systematic investigation on how the nanowire formation depends on the growth conditions.

In the literature, there are reports shown that SiO_x nanowires can be formed at high temperature with only nonreacting carry gases.[1−6] To make sure that the SiO_x nanowires formed in our experiments are not the same, we have conducted several experiments without ZnO and graphite powder mixtures. The substrate temperature was set to 1000 °C, and experiments with different argon and oxygen gas flow ratios (295 sccm of Ar and 5 sccm of O_2, 150 sccm of Ar and 150 sccm of O_2) for a duration of 30 min were carried out. We did not observe any SiO_x nanowires on any of the substrates. Therefore, our results suggest that the mixture of the ZnO and carbon powder plays a very important role in the formation of SiO_x nanowires at short growth time. Our additional experiments also found that, with only the ZnO powder, there was no SiO_x nanowire formation while, with only 2.5 g of graphite powders, the SiO_x nanowires were formed under suitable growth conditions, which demonstrated that the graphite powder was another key factor for the SiO_x nanowire formation. The detailed investigations are shown below.

2. Temperature Dependence of SiO_x Nanowire Formation. Temperature is one of the most important factors that influence the nanowire formation. For this study, we fixed the gas flow ratio (295 sccm of Ar and 5 sccm of O_2), the growth time (30 min), and the amount of graphite powder (2.5 g), and varied the furnace temperature to be 900, 950, and 1000 °C, respectively. Three different substrates, AUS, CUS, and BS, were used as well. After the experiments, the amount of graphite powder in the boats either had been greatly reduced or had totally disappeared. For both Cu and bare Si substrates, there were no nanowires formed at any of those temperatures. However, for AUS substrate, different temperatures gave different results. For $T = 900$ °C, as shown in Figure 5a, there are only Au−Si alloy islands on the entire substrate. One observes a lot of disk-shaped denude zones on the Si substrate. We did not observe any nanowire formation under the SEM examination. In fact, there are three different regions on the substrate as shown in Figure 5a: on top of the big islands, region A, is the Au−Si alloy, on the bottom of the big islands (the slope slanted into the substrate), region B, is a Si layer precipitated from Au−Si liquid alloy,[28,29] and between big islands (including the disk-shaped denude zone), region C, are numerous nanometer sized small particles, and this region is Au free.[28,29] When the temperature increases to 950 °C, the nanowires start to form as shown in Figure 5b. In general, the density of nanowires on the surface is very low, the diameter is uniform (∼50 nm), and the length of the nanorods is short (∼2−3 μm). Most of the surface is covered by the molten islands of Au−Si alloy like the ones shown in Figure 5a, while occasionally there are nanowires formed between those big Au−Si alloy islands. The network-like Si layer precipitated from the Au−Si alloy is very prominent compared to that formed at lower temperature (Figure 5a). Obviously, most of the nanowires are formed in region C (there are nanowires across region B, but they originated from region C by a close inspection), where at lower temperature it is occupied by nanometer-sized particles (Figure 5a). When the temperature increases to 1000 °C, a uniform layer of SiO_x nanowires is formed across the entire substrate as shown in Figure 5c. The low-magnification SEM image shows that there are no Au islands on the surface (at

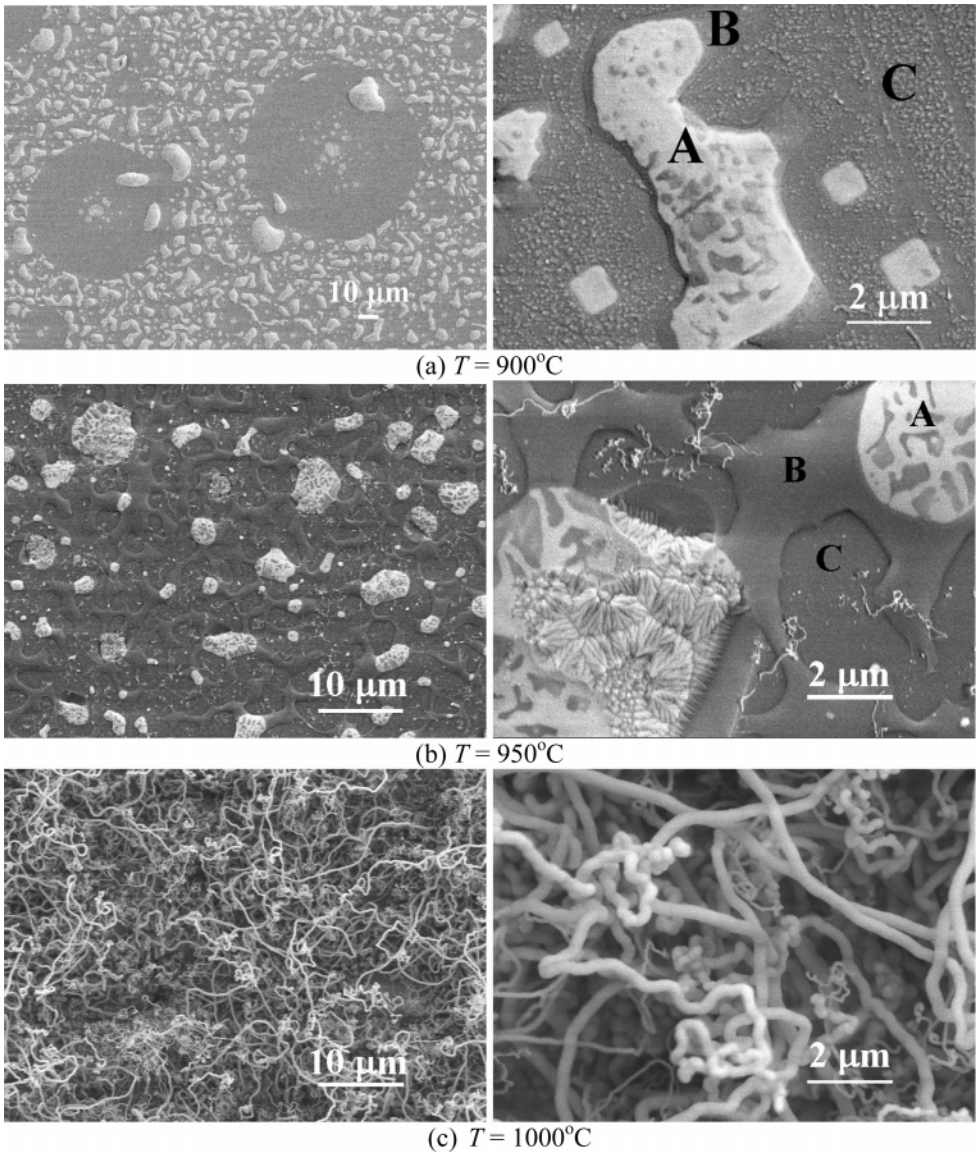

Figure 5. Representative SEM images of AUS samples prepared under different temperatures with only graphite powder as the source: (a) T = 900 °C; (b) T = 950 °C; (c) T = 1000 °C. The left panels are images with 100× magnification, and the right panels are with 10000× magnification.

least we are not able to observe any). The high-magnification SEM image shows that the diameters of the nanowires are not uniform: the diameters of the thick nanowires are about 340 nm, and those of the thin ones are about 130 nm. Higher substrate temperatures gave similar results.

3. Oxygen Flow dependence of SiO_x Nanowire Formation. During the experiments, we also found that the ratio of the Ar and O_2 flow rates played a very important role in the growth of the nanowires. A detailed study has been performed by varying the O_2 flow ratio with other fixed deposition conditions: graphite powder (2.5 g), substrate temperature (1000 °C), three different substrates (AUS, CUS, and BS), and the growth time (30 min.). After each experiment, we found that the amount of graphite powder in the quartz boat was reduced but not totally. The general trend is that, with higher O_2 flow, less graphite powder was left. We still did not observe nanowire formation on CUS and BS, but the nanowires formed on AUS changed dramatically under different O_2 flow ratios. Figure 6 shows the SEM top views of the samples prepared by different O_2 flows. Without O_2 flow (Figure 6a), there are no nanowires formed under the current conditions. With the presence of a small amount of O_2 (5 sccm, Figure 6b), there was a layer of uniform SiO_x nanowires formed on the substrates. With further increment of the O_2 flow (20 sccm), there are still nanowires formed on the substrates (Figure 6c). But unlike the nanowires formed at 5 sccm, which are uniformly across the entire substrate, the nanowires formed at 20 sccm are localized at particular surface sites. In fact, they form flower-like structures (Figure 6c): the center of the flower is an irregularly shaped hole on the substrate, while the nanowires are almost radially extended out from the hole. This kind of structure is very similar to that of SiO_x nanowires formed by Ni catalytic experiments.[17] Between those localized nanowire-formation sites, there are submicrometer-sized islands. When the O_2 flow is increased to 50 sccm, there are no long nanowires formed on the substrates. Instead, disk-shaped structures randomly appeared on the substrate with the connection of the mesh structures (Figure 6d). The larger magnification SEM image shows that the mesh structures are made of numerous short nanowires (Figure 7). The diameter of those short nanowires (~60 nm) is very uniform across the surface compared to that of the nanowires formed in Figure 6b. When the mesh structure is enlarged, one also observes a uniform network (Figure 7a). With larger magnification, as shown in Figure 7c, those short nanowires (or nanorods) are extended out from the substrate surface, and in the neighborhood of the short nanowires on the substrate, there are nanometer-

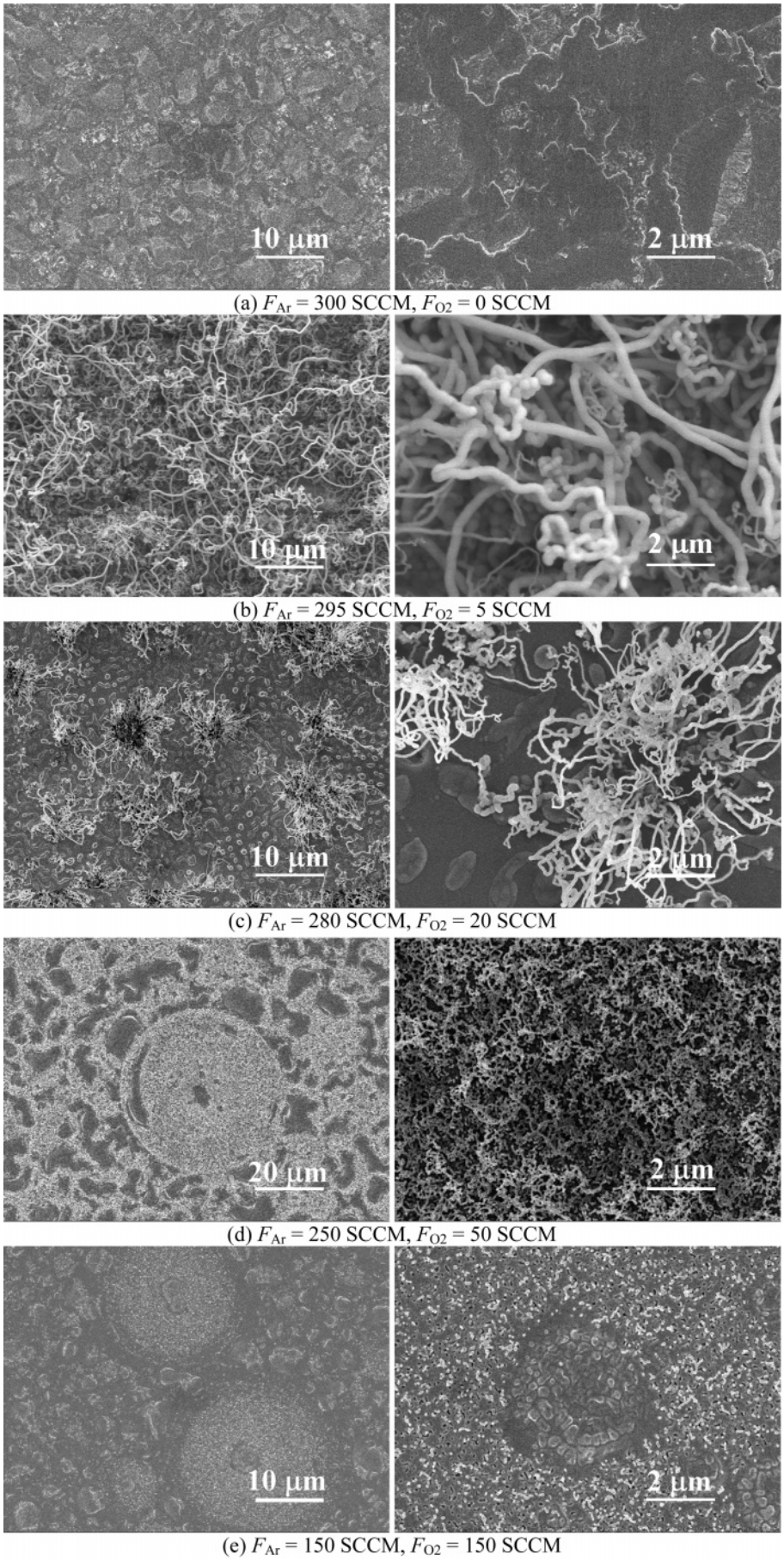

Figure 6. Representative SEM images of AUS samples prepared under different O_2 gas flow ratios with only graphite powder as the source: (a) $F_{O_2} = 0$ sccm; (b) $F_{O_2} = 5$ sccm; (c) $F_{O_2} = 20$ sccm; (d) $F_{O_2} = 50$ sccm; (e) $F_{O_2} = 150$ sccm. The left panels are images with 100× magnification, and the right panels are with 10000× magnification.

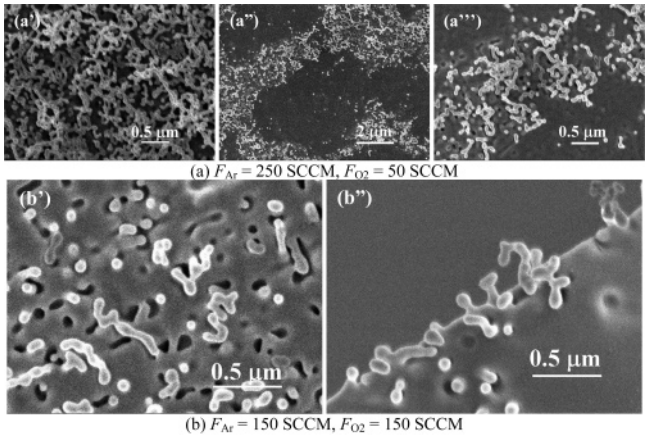

Figure 7. Representative high-magnification SEM images of AUS samples prepared under different O_2 gas flow ratios with only graphite powder as the source: (a) $F_{O_2} = 50$ sccm; (b) $F_{O_2} = 150$ sccm.

sized holes. It is interesting to notice that, Figure 6d is very similar to Figure 5a, except that they are reversed: the white region in Figure 6d seems to correspond to the region between the Au−Si alloy islands (region C) in Figure 5a, while the dark region in Figure 6d corresponds to the Au−Si alloy islands in Figure 5a (Regions A and B). It is reasonable to believe that those nanoparticles on the surface in Figure 5a (region C) are the possible source or nucleation centers for the formation of those short nanowires. When the O_2 flow increases further (150 sccm), one still observes the disk-shaped morphology (Figure 6e), which is similar to that of Figure 6d. However, in this case, there is no network of short nanowire structures formed. Instead, the white area in Figure 6e is covered with nanometer-sized holes and rods (Figure 6e, right panel). Higher magnification SEM images shown in Figure 7 clearly demonstrate the relationship between the nanohole and nanorod. In most cases, a nanorod is associated with an adjacent nanohole. Some of the nanorods are bridging across the nanoholes. It appears in the SEM images that the nanorods have smooth surfaces, and the tips of the rods take an elliptical shape. Some of the shorter rods even have a spherical shape, like a melting droplet. The diameter of the nanorod is very uniform, ~60 nm. The cross-section view in Figure 7 shows that the nanorods grow from the substrate surface. It seems that the formation of the nanorod is due to material precipitation from the Si substrate. With a higher O_2 flow ratio, the formation of long SiO_x nanowires has been suppressed, and the morphology of the surface under higher O_2 flow ratio resembles the initial growth stages for SiO_x nanowires.

From both the temperature- and O_2-flow-dependent studies we noticed that the optimum conditions for long uniform SiO_x nanowire growth are 1000 °C substrate temperature, 250 sccm of Ar, and 5 sccm of O_2.

4. Time Dependence of SiO_x Nanowire Formation. We have also studied how the nanowires grow as a function of time under the optimum growth conditions mentioned in the above section. Figure 8 shows the corresponding SEM images for $t =$ 2, 5, 10, 20, and 30 min. It is interesting to notice that, for $t =$ 2 min, one can still observe Au−Si alloy islands (the inset SEM picture in the left-bottom corner of Figure 8a), while the nanowires are only grown between those islands. In general, there are two trends: First, the surface coverage of nanowires on the substrate increases with growth time. For $t = 2$ and 5 min (Figure 8a,b), parts of the substrate are not covered by the nanowires, while, for $t = 10$, 20, and 30 min (Figure 8c−e), it is very hard to observe the underlying substrate due to the very dense nanowires on top of the substrate. Second, the diameters of the nanowires increase with growth time as well. For the higher magnification SEM images in the right panels (Figure 8), we observe that, at a shorter growth time, the diameters of the nanowires are quite uniform (Figure 8(a,b) while, at a longer growth time, the sizes of the nanowires are different: there are many nanowires with a diameter around 100 nm, while others are larger than 200 nm. We have performed statistical measurements of the diameter of the nanowires on all the samples. Figure 9a shows the dependence of nanowire size on the growth time. For $t > 5$ min, the size of the nanowire obeys a binomial distribution. An example of the binomial distribution for the sample grown for $t = 30$ min is plotted in Figure 9b. The scattered symbols are the experimental data, and the solid curves are the best fits by two Gaussian functions. The center positions of two Gaussian functions are the two average diameters that characterize the different nanowire sizes shown in SEM images. The general trend in Figure 9a shows that the diameters of the nanowires increase almost monotonically with growth time. Another important parameter for nanowire growth is the length of the wires. Due to the entanglement of the nanowires on the substrate (Figure 9), we cannot estimate the exact value of the length.

It is also interesting to notice that at initial growth stages ($t = 2$, 5, and 10 min) there are pits formed on the substrates. It appears, by the SEM images, that the pits for $t = 5$ min are smaller, denser, and deeper, compared to those for $t = 2$ min. Those pits are actually associated with the growth mechanism, which we will discuss in the next section.

IV. Discussion

The major observations in the Experimental Section can be summarized as follows: (1) Carbon was the source for promoting the formation of SiO_x nanowires. (2) The formation of SiO_x nanowires needed a thin Au film. (3) The growth of SiO_x nanowires was suppressed both without the O_2 gas stream and with a high ratio of O_2 gas. (4) The diameter of the SiO_x nanowires increased monotonically with growth time. (5) The mixture of ZnO and graphite powders lowered the SiO_x nanowire formation temperature. These observations have illustrated the nanowire growth mechanism from different aspects. One of the major conclusions from the above experiments is that the graphite powder plays an important role in the formation of the SiO_x nanowires. Specifically, according to the arguments below, we concluded, from our experimental results, that CO may play a dominant role in accelerating nanowire growth.

Since the graphite powders were placed in the upstream, with the incoming O_2 gas, the powders were first oxidized through the following reactions:[30]

$$2C + O_2 \rightleftarrows 2CO \quad (2)$$

$$C + O_2 \rightleftarrows CO_2 \quad (3)$$

$$2CO + O_2 \rightleftarrows 2CO_2 \quad (4)$$

We observed that the amount of graphite powder that remained on the boat was greatly reduced, but not totally consumed by the oxidation. This demonstrates that graphite has changed into its oxide forms, CO and CO_2. The O_2-flow-ratio-dependent experiments showed that only with an appropriately small O_2 flow were nanowires formed uniformly on the substrate while, with more O_2, the nanowire formation was suppressed. In terms of chemical reactions 2−4, the increased O_2 flow ratio will

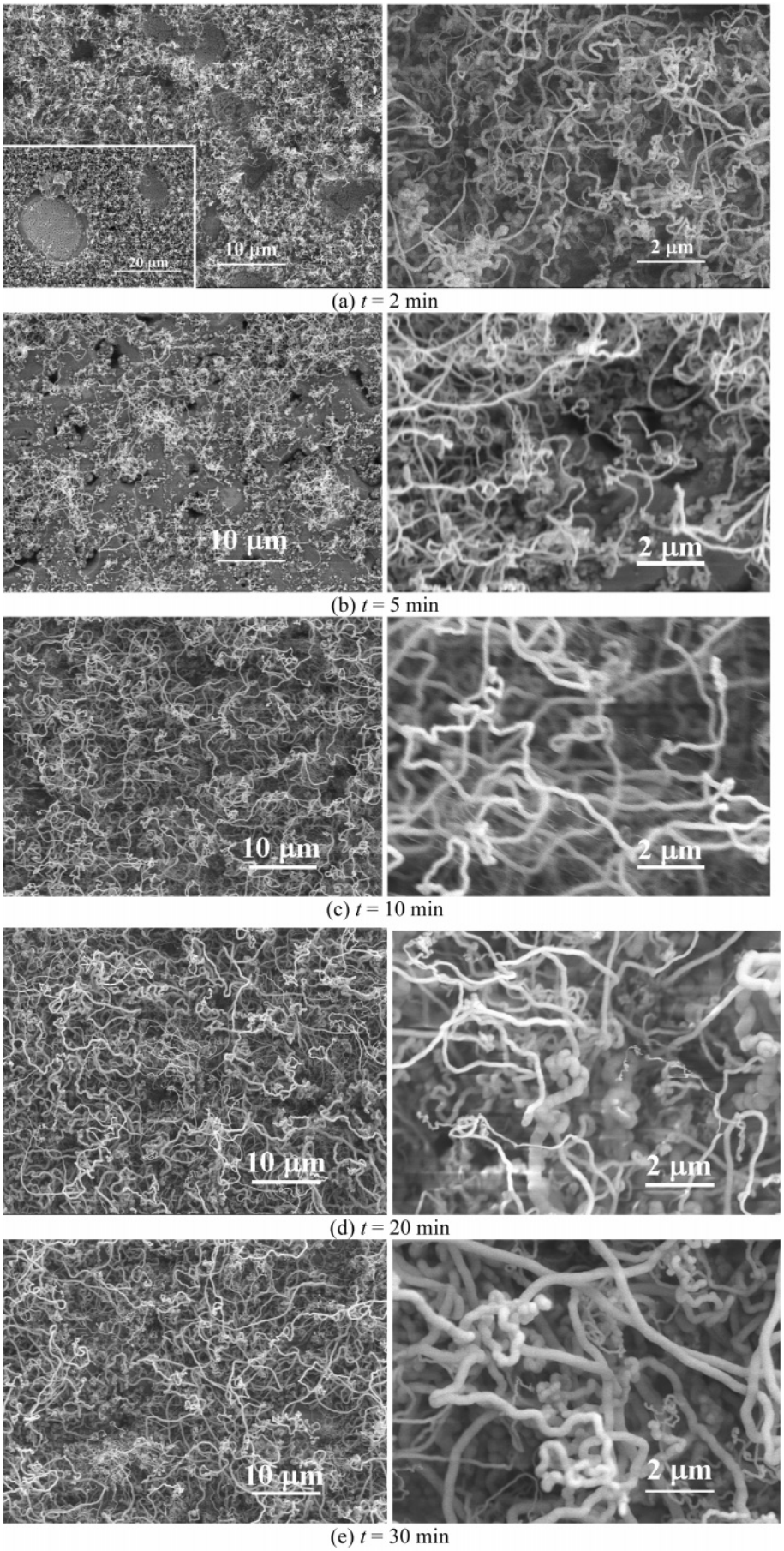

Figure 8. Representative SEM images of AUS samples prepared under different growth times with only graphite powder as the source: (a) t = 2 min; (b) t = 5 min; (c) t = 10 min; (d) t = 20 min; (e) t = 30 min. The left panels are images with 100× magnification, and the right panels are with 10000× magnification.

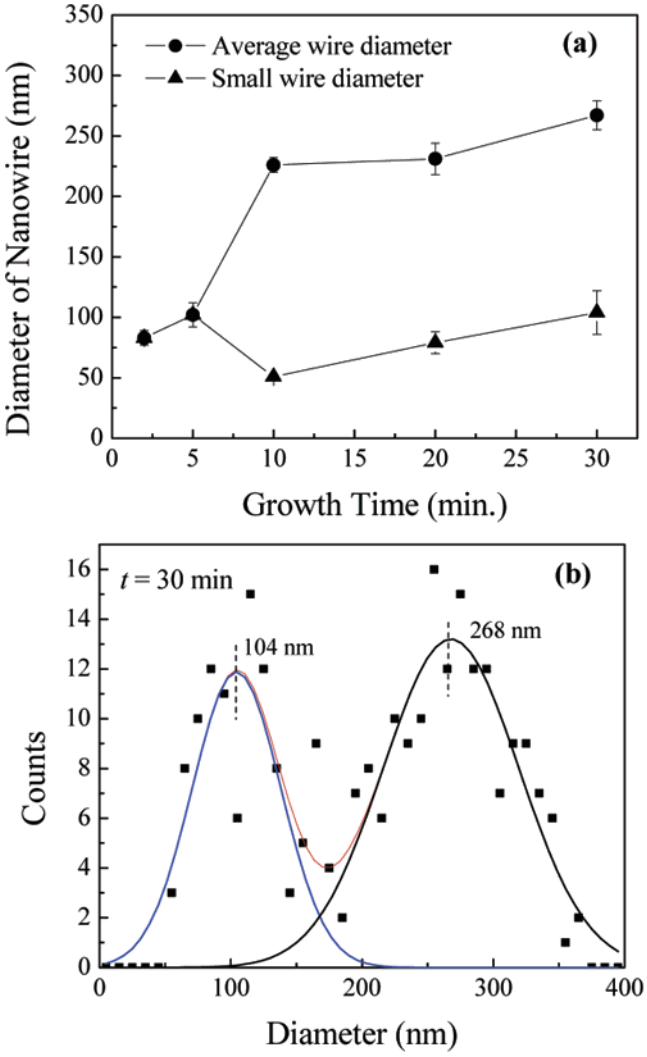

Figure 9. (a) Diameter of the nanowire versus the growth time. (b) Distribution of the diameter of the nanowires for $t = 30$ min.

induce two major effects: first, to benefit reaction 3, i.e., to generate more CO_2, at the expense of CO; second, to accelerate the oxidation speed (which could consume all the graphite powder before the end of the experiments). The second effect is not a major issue for our experimental conditions since in most cases we observed extra graphite powder left unreacted. If CO_2 played the dominant role as described by eq 1, with more O_2 flow, due to reactions 3 and 4, one should expect more SiO_x nanowires on the substrates, which would be in opposition to the experimental observations. In addition, the SiO_x nanorod formed at very high O_2 flow (Figure 7) showed that the nanowires came out from the substrate, not from the vapor phase. Therefore, we concluded that CO plays a major role. To confirm this speculation, we conducted several test experiments with a mixture flow of Ar (250, 290, 295 sccm) and CO (50, 10, 5 sccm, respectively), under the same growth conditions but without the graphite powder (substrate temperature 1000 °C, three different substrates, AUS, CUS, and BS, and total growth time 30 min), and we have also observed white fluffy nanowires formed on AUS substrates.

The next question is how CO is involved in the formation of SiO_x nanowires. Before answering this question, we would like to see, in our case, what the possible growth mechanism for the nanowires could be. All the experiments with successful SiO_x nanowire formation required the presence of a Au thin film on the substrate. This requirement generally leads to a VLS growth mechanism. For example, several reports on Au thin film based SiO_x nanowires have claimed the VLS growth mechanism.[7−9] However, in our experiments, both XPS and EDX measurements did not observe any trace of Au on the tips of the nanowires or on the surface of the samples, which indicates that the formation of the SiO_x nanowires does not follow the VLS mechanism. In fact, the high O_2 flow results (Figure 7) are very intriguing, and we believe they represent the very initial stages of the nanowire formation: the wires are formed between the big eutectic Au−Si islands, and the source of the wire is from the substrate, not from the vapor. Recently, Paulose et al. have studied the formation of Au−SiO_x composite nanowires under similar conditions without graphite powder, and they pointed out that the growth mechanism was due to a so-called solid−liquid−solid process: Si atoms diffused to the Au−Si liquid alloy from the substrate, and precipitated from the alloy to form nanowires.[31] The evidence for such a speculation was that pits were created on the Si surface after the SiO_x nanowires were removed by HF. We have also observed pits formed on the substrate (Figure 8). To make sure our cases belong to this growth mechanism, we have also dipped three time-dependent samples, $t = 2$, 10, and 30 min, into HF (49%) for 20 h in order to completely remove the oxide layer and SiO_x nanowires on the surface. Figure 10 shows the top-view SEM images of each surface for three different magnifications: 200×, 1000×, and 10000×. For $t = 2$ min (Figure 10a), we have observed disk-shaped denude zones and Au−Si alloy islands, which are very similar to those of Figure 5a,b. Between the disks, there are mixtures of square-shaped pits and big irregularly shaped holes filled with a white substance (appearing in the SEM images). Those irregular holes correspond to the Au−Si alloy islands present in Figure 5. Compared to Figure 8a (with SiO_x nanowires on the surface), it is very clear that the nanowires are only grown between the big Au−Si islands, e.g., in the locations of the small square pits shown in Figure 10a″, as well as in the denude zones. We also notice that the Au−Si islands (the white parts in Figure 10a) actually sink/diffuse into the substrate instead of protruding from the surface as shown in Figures 5a,b. When $t = 10$ min, the etched surface also exhibits many disk-shaped denude zones (Figure 10b′). But compared to that at $t = 2$ min, the density of the disk-shaped denude zones increased, and one cannot observe any distinct Au−Si eutectic islands similar to those in Figure 10a (Figure 10b′,b″). In fact, the regions between the denude zones became very rough, and covered with many irregular holes. By further zooming in on some of the holes, we still observe the Au−Si alloys (the white area) (Figure 10b‴), but the amount of the Au−Si in the hole has been greatly reduced. Associated with the Au−Si alloys are very deep holes on the surface. When the growth time t increases to 30 min, the etched substrate shows a very different morphology: the etched substrate becomes very smooth as compared to the previous two (Figure 10c′). Even at very high magnification, one can only observe small square-shaped pits, and the surface is almost free of the irregular holes. There are no signs of Au−Si alloy islands on the surface as shown in Figure 10a,b. It seems that, to produce more nanowires, the Au or Au−Si alloys have to diffuse into the Si wafer and create holes in the surface. To further confirm this observation, we also performed cross-section SEM on the sample with $t = 10$ min. As shown in Figure 11, there is a highly undulated interface between the nanowire layer and the substrate. Some of the undulations are holes that even extend very deeply into the substrate (Figure 11a). Although we cannot tell from the SEM images the quality of the interfacial layer,

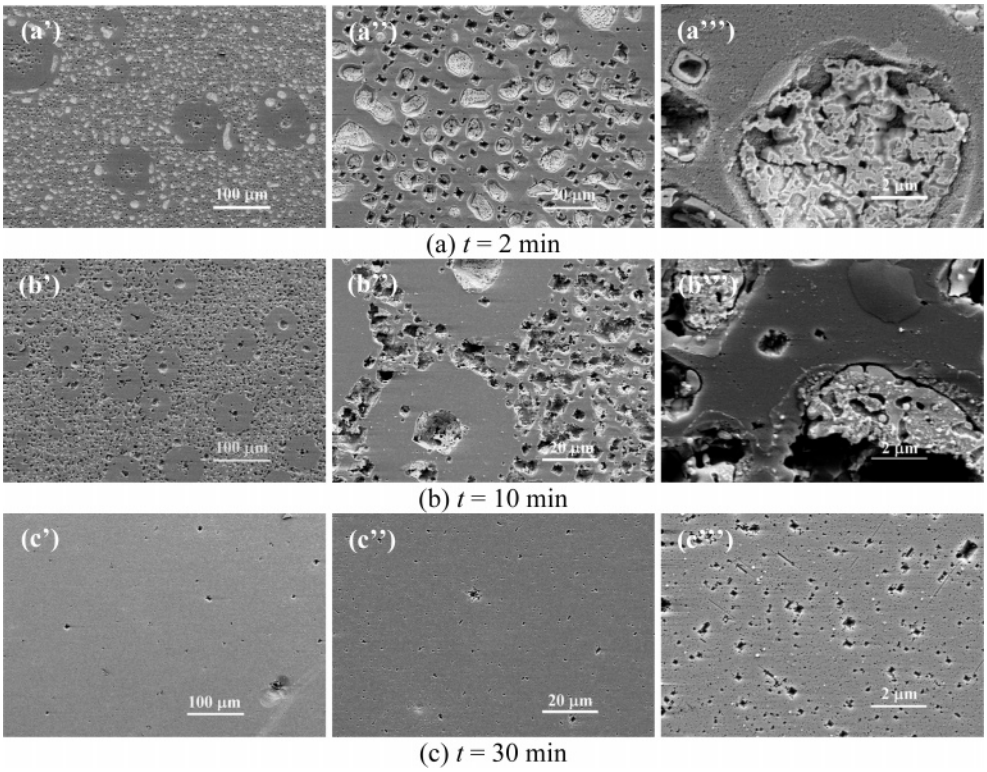

Figure 10. Representative SEM images of AUS samples dipped in HF for different growth times: (a) $t = 2$ min; (b) $t = 10$ min; (c) $t = 30$ min. The left panels are images with 200× magnification, the middle panels are with 1000× magnification, and the right panels are with 10000× magnification.

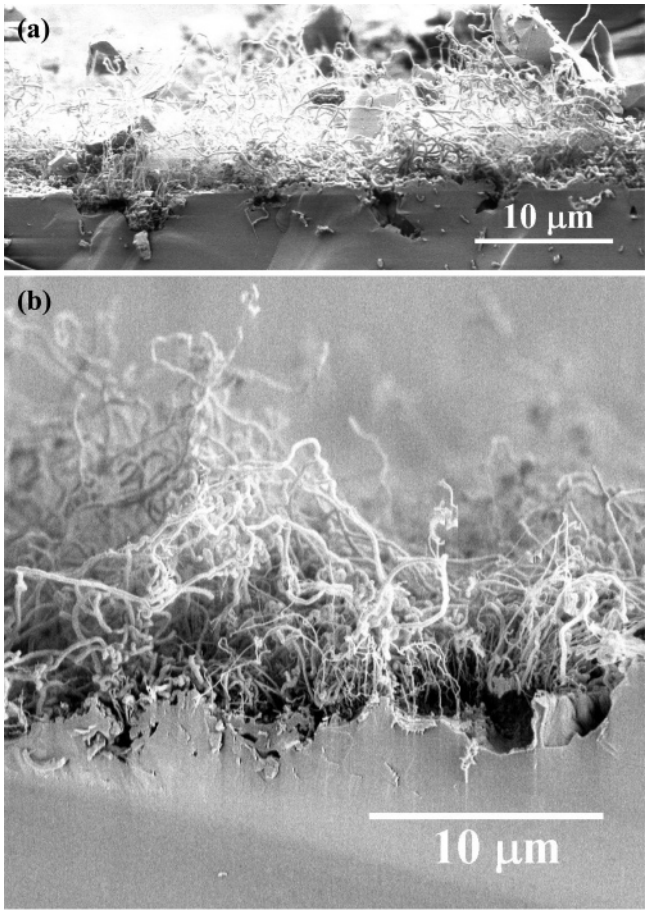

Figure 11. Cross-section SEM images of a nanowire sample for the growth time $t = 10$ min.

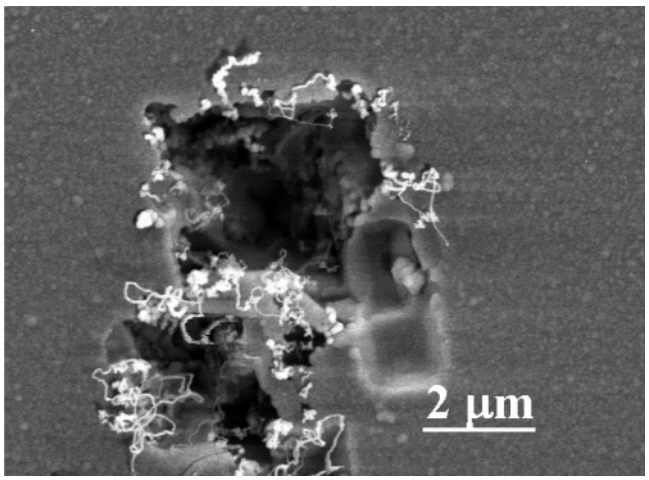

Figure 12. Nanowires formed in the pit on Cu−Si substrate.

the randomness and the voids in Figure 11b imply that the crystalline quality of the top surface of the substrate (the interface) is much worse than that of the as-received Si wafer. In Figure 11b, one also observes that the nanowires are rooted from the substrate. The above results demonstrate further that the growth mechanism is not a VLS process (no pits are expected for the VLS process). In fact, the results from Figures 6, 7, 10, and 11 are consistent with each other, and suggest that the SiO_2 nanowires are grown in the Au-free regions, and the nanowire growth is always associated with the pit formation. By examining the pits in CUS samples very carefully, occasionally we also observe a few nanowires, as shown in Figure 12. The nanowires are grown around the pits or inside the pits. Pitting into the substrate is an important process to form SiO_x nanowires under the current growth conditions. The round or elliptical shapes of the tips of the nanorods (Figure 7) suggest that the initial growth of the nanowires starts from a melt. This

conclusion can be further backed up by some CUS samples. All this evidence points to a solid−liquid−solid growth mechanism. One of the roles that Au may play is to make a highly stressed Si surface layer for pitting to occur. Furthermore, Au is also an excellent catalyst for CO oxidation.[32,33] When CO molecules in the gas phase hit the substrate at high temperature, the CO molecules will react with O_2 to form CO_2, and release energy on the Au−Si islands and vicinities. They heat local areas and generate local temperature gradients. This might be the reason we observe nanowire formation in a short time and at relatively low temperature compared to that in most work in the literature.

The diameter of the nanowire increasing as a function of the growth time is an observation that is very hard to understand. The binomial distribution was only observed after a relatively long growth time ($t \geq 10$ min), which suggests the later growth stage of the nanowire is different from the initial stage. One of the suspicions is that the quartz boat or tube may react with graphite or CO_2, and generate gas-phase SiO. The SiO will coat onto the SiO_x nanowires through a mechanism similar to chemical vapor deposition. Currently, we do not have the facility to test this speculation.

IV. Conclusions

In conclusion, during the attempt to fabricate ZnO nanowires, we found a way to fabricate SiO_x nanowires on Au-coated Si substrate. The formation of the SiO_x nanowires depends on a series of experimental conditions, such as substrate coating (Au), the presence of graphite powder, the substrate temperature, the oxygen flow, and the growth time. The optimum growth conditions in this study are a substrate temperature of 1000 °C, an Ar flow of 250 sccm, and an O_2 flow of 5 sccm. The systematic investigation on the effect of growth temperature, oxygen flow rate, and growth time on the growth of the SiO_x nanowires has suggested that the formation of SiO_x nanowires may be due to a so-called solid−liquid−solid mechanism.

Acknowledgment. This work is supported by The University of Georgia Research Foundation Junior Faculty Research Fund and the National Science Foundation (ECS-0304340). We also thank J.-G. Fan and X.-J. Tang for their help with the SEM measurements, and Samuk Pimanpang, F. Tang, and G.-C. Wang at RPI for their help with the XPS measurements. We thank Mr. Stephen Chaney for proofreading the manuscript.

References and Notes

(1) Peng, X. S.; Wang, X. F.; Zhang, J.; Wang, Y. W.; Sun, S. H.; Meng, G. W.; Zhang, L. D. *Appl. Phys. A* **2002**, *74*, 831.

(2) Dai, L.; Chen, X. L.; Zhou, T.; Hu, B. Q. *J. Phys.: Condens. Matter.* **2002**, *14*, L473.

(3) Dai, L.; Chen, X. L.; Jian, J. K.; Wang, W. J.; Zhou, T.; Hu, B. Q. *Appl. Phys. A* **2003**, *76*, 625.

(4) Hu, J. Q.; Jiang, Y.; Meng, X. M.; Lee, C. S.; Lee, S. T. *Chem. Phys. Lett.* **2003**, *367*, 339.

(5) Meng, G. W.; Peng, X. S.; Wang, Y. W.; Wang, C. Z.; Wang, X. F.; Zhang, L. D. *Appl. Phys. A* **2003**, *76*, 119. Lee, K.-H.; Lee, S.-W.; R. R. Vafleet; Sigmund, W. *Chem. Phys. Lett.* **2003**, *376*, 498.

(6) Wang, Z. L.; Gao, R. P.; Cole, J. L.; Stout, J. D. *Adv. Mater.* **2000**, *12*, 1938.

(7) Liu, Z. Q.; Xie, S. S.; Sun, L. F.; Tang, D. S.; Zhou, W. Y.; Wang, C. Y.; Liu, W.; Li, Y. B.; Zou, X. P.; Wang, G. *J. Mater. Res.* **2001**, *16*, 683.

(8) Wang, Y. W.; Liang, C. H.; Meng, G. W.; Peng, X. S.; Zhang, L. D. *J. Mater. Chem.* **2002**, *12*, 651.

(9) Paulose, M.; Varghese, O. K.; Grimes, C. A. *J. Nanosci. Nanotechnol.* **2003**, *3*, 341.

(10) Yu, D. P.; Hang, Q. L.; Ding, Y.; Zhang, H. Z.; Bai, Z. G.; Wang, J. J.; Zou, Y. H.; Qian, W.; Xiong, G. C.; Feng, S. Q. *Appl. Phys. Lett.* **1998**, *73*, 3076.

(11) Chen, Y.-J.; Li, J.-B.; Dai, J.-H. *Chem. Phys. Lett.* **2001**, *344*, 450.

(12) Wu, X. C.; Song, W. H.; Wang, K. Y.; Hu, T.; Zhao, B.; Sun, Y. P.; Du, J. J. *Chem. Phys. Lett.* **2001**, *336*, 53.

(13) Chen, Y. J.; Li, J. B.; Han, Y. S.; Wei, Q. M.; Dai, J. H. *Appl. Phys. A* **2002**, *74*, 433.

(14) Zhang, H.-F.; Wang, C.-M.; Buck, E. C.; Wang, L.-S. *Nano Lett.* **2003**, *3*, 577.

(15) Takikawa, H.; Yatsuki, M.; Sakakibara, T. *Jpn. J. Appl. Phys.* **1999**, *38*, L401.

(16) Carter, P.; Gleeson, B.; Young, D. J. *Oxid. Met.* **2001**, *56*, 375.

(17) Zhang, Z. J.; Ramanath, G.; Ajayan, P. M.; Goldberg, D.; Bando, Y. *Adv. Mater.* **2001**, *13*, 197.

(18) Zheng, B.; Wu, Y. Y.; Yang, P. D.; Liu, J. *Adv. Mater.* **2002**, *14*, 122.

(19) Pan, Z. W.; Dai, Z. R.; Ma, C.; Wang, Z. L. *J. Am. Chem. Soc.* **2002**, *124*, 1817.

(20) Wang, J. C.; Zhan, C. Z.; Li, F. G. *Solid State Commun.* **2003**, *125*, 629.

(21) Ma, R.; Bando, Y. *Chem. Phys. Lett.* **2003**, *377*, 177.

(22) Wagner, R. S.; Ellis, W. C. *Appl. Phys. Lett.* **1964**, *4*, 89.

(23) Zhu, Y. Q.; Hsu, W. K.; Terrones, M.; Grobert, N.; Terrones, H.; Hare, J. P.; Kroto, H. W.; Walton, D. R. M. *J. Mater. Chem.* **1998**, *8*, 1859.

(24) Saulig-Wenger, K.; Cornu, D.; Chassagneux, F.; Epicier, T.; Miele, P. *J. Mater. Chem.* **2003**, *13*, 3058.

(25) Huang, M. H.; Wu, Y.; Feick, H.; Tran, N.; Weber, E.; Yang, P. *Adv. Mater.* **2001**, *13*, 113.

(26) Yao, B. D.; Chan, Y. F.; Wang, N. *Appl. Phys. Lett.* **2002**, *81*, 757.

(27) Li, S. Y.; Lee, C. Y.; Tseng, T. Y. *J. Cryst. Growth* **2003**, *247*, 357.

(28) Wakayama, Y.; Tanaka, S.-I. *Surf. Sci.* **1999**, *420*, 190.

(29) Ressel, B.; Prince, K. C.; Heun, S.; Homma, Y. *J. Appl. Phys.* **2003**, *93*, 3886.

(30) *CRC Handbook of Chemistry and Physics*, 59th ed.; CRC Press: Boca Raton, FL, 1978.

(31) Paulose, M.; Varghese, O. K.; Grimes, C. A. *J. Nanosci. Nanotechnol.* **2003**, *3*, 341.

(32) Guczi, L.; Petoe, G.; Beck, A.; Frey, K.; Geszti, O.; Molnar, G.; Daroczi, C. *J. Am. Chem. Soc.* **2003**, *125*, 4332.

(33) Boyen, H.-G.; Kaestle, G.; Weigl, F.; Koslowski, B.; Dietrich, C.; Ziemann, P.; Spatz, J. P.; Riethmueller, S.; Hartmann, C.; Moeller, M.; Schmid, G.; Garnier, M. G.; Oelhafen, P. *Science* **2002**, *297*, 1533.